Electronic Structure of Gadolinium Calcium Oxoborate

A. Nelson, J. Adams, K. Schaffers

July 2, 2004

Disclaimer

This document was prepared as an account of work sponsored by an agency of the United States Government. Neither the United States Government nor the University of California nor any of their employees, makes any warranty, express or implied, or assumes any legal liability or responsibility for the accuracy, completeness, or usefulness of any information, apparatus, product, or process disclosed, or represents that its use would not infringe privately owned rights. Reference herein to any specific commercial product, process, or service by trade name, trademark, manufacturer, or otherwise, does not necessarily constitute or imply its endorsement, recommendation, or favoring by the United States Government or the University of California. The views and opinions of authors expressed herein do not necessarily state or reflect those of the United States Government or the University of California, and shall not be used for advertising or product endorsement purposes.

Electronic Structure of Gadolinium Calcium Oxoborate

A. J. Nelson, J.J. Adams, and K. I. Schaffers
Lawrence Livermore National Laboratory, Livermore, CA 94550 USA

Abstract

Gadolinium calcium oxoborate (GdCOB) is a nonlinear optical material that belongs to the calcium–rare-earth (R) oxoborate family, with general composition $Ca_4RO(BO_3)_3$ (R^{3+} = La, Sm, Gd, Lu, Y). X-ray photoemission was applied to study the valence band electronic structure and surface chemistry of this material. High resolution photoemission measurements on the valence band electronic structure and Gd $3d$ and $4d$, Ca $2p$, B $1s$ and O $1s$ core lines were used to evaluate the surface and near surface chemistry. These results provide measurements of the valence band electronic structure and surface chemistry of this rare-earth oxoborate.

Introduction

Gadolinium calcium oxoborate (GdCOB) is a nonlinear optical (NLO) material that belongs to the calcium–rare-earth (R) oxoborate family, with general composition $Ca_4RO(BO_3)_3$ (R^{3+} = La, Sm, Gd, Lu, Y). [1-3] The nonlinear properties of these crystals have been measured and these NLO materials are found to have potential for high-average power frequency conversion and intra-cavity doubling. [4,5]

The optical properties of borate crystals appear to be related to their molecular structure. These crystals are constructed from a basic structure unit: $(BO_3)^{3-}$ anionic groups. The anionic group is thought to determine the NLO coefficient of borate crystals according to the anionic group theory [6]. If the dangling bonds of the three terminated oxygen atoms of the $(BO_3)^{3-}$ groups are interlinked with cations, an absorption edge appearing at wavelengths as short as 155 nm is also possible.

GdCOB crystallizes in the monoclinic biaxial crystal system belonging to the *Cm* space group, and the number of formula units is $Z = 2$. [7,8] GdCOB is isostructural to the calcium fluoroborate $Ca_5(BO_3)_3F$, which is related to the common fluoroapatite structure $Ca_5(PO_4)_3F$. [9,10]

There are two types of Ca^{2+} ions that occupy distorted octahedral sites. All octahedra share corners with BO_3 triangles to form a three-dimensional network. There are two kinds of boron site, B(1) and B(2), with threefold coordination. The planar borate unit lies approximately parallel to the (001) plane.

The Gd^{3+} ions are located in the crystallographic mirror plane (Fig. 1). The environment of Gd^{3+} ion is a distorted octahedron with *Cs* site symmetry. Four oxygen ions are shared with the BO_3 groups. One should also consider the existence of a probable disorder

between calcium and gadolinium atoms in the two octahedral positions. [7,8]

This paper presents results from an investigation of the composition and the electronic structure of this rare-earth calcium oxoborate. Core-level spectroscopy and results for the occupied states in the valence band are the first comprehensive measurements for this material.

Experimental

The GdCOB compound was prepared by classical solid-state reaction, with Gd_2O_3, $CaCO_3$, and B_2O_3 in stoichiometric proportions. The mixture was heated at 950 °C for 18 h, cooled and ground, and then heated again at 1350 °C for 24 h. The x-ray diffraction patterns confirmed that the compound was a single phase.

Large crystals of GdCOB, grown by the Czochralski method, were obtained through careful alignment of the seed crystal along the preferred growth direction (the dielectric axis). This material melts congruently, and crystals were grown while rotating at 20 rpm with a pull rate of 1 mm/h from a 7.62-cm diameter iridium crucible. Typical growth sizes were 25 mm diameter x 50 mm in length. The crystals were clear, with minimal bubble core defects perpendicular to the [010] growth direction. The location of the dielectric axis was determined by x-ray diffraction, and 1-mm thick samples were cut for analysis. GdCOB was found to be transparent between 320 and 2600 nm.

X-ray photoemission spectroscopy (XPS) was performed using a focused monochromatic Al K x-ray (1486.7 eV) source for excitation and a spherical section analyzer. The instrument has a 16-element multichannel detection system. A 1 mm diameter x-ray beam was used for analysis. The x-ray beam is incident normal to the sample and the x-

ray detector is at 45° away from the normal. The pass energy was 23.5 eV giving an overall energy resolution of 0.3 eV. The collected data were referenced to an energy scale with binding energies for Cu $2p_{3/2}$ at 932.72± 0.05 eV and Au $4f_{7/2}$ at 84.01± 0.05 eV. Surface contamination was removed by sputter etching with 1 kV Ar^+ ions prior to XPS compositional analysis. Low energy electrons and argon ions were used for specimen neutralization.

Results and Discussion

The 3d core-level photoemission final state configuration for trivalent rare earths exhibits a doublet structure due to bonding and antibonding states that become less resolved as one progresses through the lanthanide series. Specifically, the core-level final state configuration can be either $3d^94f^N$ or $3d^94f^{N+1}\underline{L}$ due to final state screening effects, where $\underline{L}$ indicates that there is one electron missing in the ligand valence state, e.g. O 2p hole. This is in addition to the fact that the $3d_{5/2,3/2}$ spin-orbit components are separated by 10's of eV.

Figure 2(a) presents the high-resolution Gd $3d_{5/2,3/2}$ core-level spectra for the GdCOB crystal and Gd-oxide model compound. The final state for Gd is unique due to the occupied 5d itinerate level, i.e. final state configuration $3d^94f^75d^1$ or $3d^94f^75d^2\underline{L}$. The Gd $3d_{5/2,3/2}$ spin-orbit pair is separated by 32.2 eV and the $3d_{5/2}$ peak has a full-width-half-maximum (FWHM) of 5.6 eV indicative of multiple bonding states. The typical doublet structure observed for other rare earths, and due to bonding and antibonding states between final state configurations, is not resolved for trivalent Gd. [11-13] The smaller energy difference indicates a higher degree of mixing between these two states and the core-valence intra-atomic exchange is dominated by the $3d$ core-$4f$ exchange interaction.

The high-resolution Gd $4d_{5/2,3/2}$ photoemission spectra in Figure 2(b) for the GdCOB

crystal and Gd-oxide model compound shows the manifestation of the *p-f* bonding-antibonding states as indicated by the broad $4d_{5/2,3/2}$ spin-orbit pair. Multiplet structures due to the Gd 4*d*-4*f* interaction are also included in the spectrum envelope. Note that it has been shown that the 4*d*–4*f* interaction is as strong as the 4*d* spin-orbit coupling. [14]

The B 1*s* binding energy from the core-level spectra shown in Figure 3(a) is 193.3 eV for the B_2O_3, in agreement with the literature. [15,16] The boron in GdCOB exhibits less of a chemical shift and has a B 1*s* binding energy of 192.0 eV. This can be explained by first noting that each B atom in the GdCOB unit cell is coordinated with three O atoms forming BO_3 triangles in a three-dimensional network at two sites in the GdCOB lattice. However, the B at these sites shares oxygen with the Ca and Gd complexes, and the Ca-O bond is predominantly ionic. Thus, the majority of the oxygen charge is shared not with the B, but with the Ca.

Figure 3(b) presents the O 1*s* core-level spectra for the GdCOB and the model oxide compounds. The measured O 1*s* binding energies for Gd_2O_3 and B_2O_3 are comparable to literature values. [16,17] The full-width-half-maximum (FWHM) of the O 1s peak for the GdCOB is 2.6 eV, and for the peak representing Gd-O bonding in Gd_2O_3 is 2.4 eV. Oxygen is bonded to Gd, Ca and B in the GdCOB unit cell and thus the larger FWHM is expected.

The valence band (VB) spectra for the GdCOB crystal and model compounds are presented in Figure 4. The upper valence bands are composed primarily of overlapping Gd 4*f*, B and O 2*p* states that hybridize with the occupied Gd 5*d* states near the valence band maximum. Specifically, the Gd 4*f* peak maximum is located at 9.2 eV below the valence band edge whereas Gd 5*d* electrons contribute at the crystal valence band edge. [18,19] The higher binding energy Gd 5*p*, Ca 3*p* and O 2*s* core-level peaks are also shown in this figure. Note

that the O $2s$ band fills in the gap between Gd $5p$ spin-orbit pair for Gd_2O_3. Mixing of the Gd $5p$, Ca $3p$ and O $2s$ lower valence band states in GdCOB is more pronounced than previous results for LaCOB. [20] In addition, Gd $5p$ multiplet splitting will be more strongly influenced by the covalency and ligand coordination of the $Gd^{3+}O_6^{n-}$ groups.

Conclusions

X-ray photoemission (XPS) spectroscopy was used to examine the electronic structure of gadolinium calcium oxoborate. XPS results for the occupied states showed a high degree of mixing between the p-f bonding-antibonding states. The valence bands are dominated by overlapping Gd $4f$ and O $2p$ states that hybridize with the occupied Gd $5d$ states near the valence band maximum.

Acknowledgements

References

1. R. Norrestam, M. Nygren, and J. O. Bovin, Chem. Mater. **4**, 737 (1992).

2. G. Aka, A. Kahn-Harari, D. Vivien, J. M. Benitez, F. Salin, and J. Godard, Eur. J. Solid State Inorg. Chem. **33**, 727–736 (1996).

3. Takatomo Sasaki, Yusuke Mori, Masashi Yoshimura, Yoke Khin Yap, and Tomosumi Kamimura, Materials Science and Engineering 30, 1 (2000).

4. G. Aka, A. Kahn-Harari, F. Mougel, D. Vivien, F. Salin, P. Coquelin, P. Colin, D. Pelenc and J. P. Damelet, J. Opt. Soc. Am. **B14(9)**, 2238 (1997).

5. J. J. Adams, C. A. Ebbers, K. I. Schaffers, and S. A. Payne, Opt. Lett. **26**, 217 (2001).

6. C. Chen, in: Laser Science and Technical International Handbook, Vol. 15, Harwood, New York, 1993.

7. A. B. Ilyukhin and B. F. Dzhurinskii, Russ. J. Inorg. Chem. **38**, 847 (1993).

8. A. Pajaczkowska, A. Klos, B. Hilczer, N. Menguy, and A. Novosselov, Cryst. Growth Des. 1(5), 363 (2001).

9. Lei Shirong, Huang Qingzhen, Zheng Yifan, Jiang Aidong, and Chen Chuangtian, Acta Crystallogr. Sect. C **45**, 1861 (1989).

10. J. G. Fletcher, F. P. Glasse, and A. Howie, Acta Crystallogr. Sect. C **47**, 12 (1991).

11. D. F. Mullica, C.K.C. Lok , H.O. Perkins, G.A. Benesh, V. Young, J. Electron Spectroscopy and Related Phenomena **71**, 1 (1995).

12. Andrei Novosselov, Ewa Talik, Anna Pajaczkowska, J. Alloys and Compounds **351**, 50 (2003).

13. Chikashi Suzuki, Jun Kawai, Masao Takahashi, Aurel-Mihai Vlaicu, Hirohiko Adachi, Takeshi Mukoyama, Chem. Phys. **253**, 27 (2000).

14. S.P. Kowalczyk, N. Edelstein, F.R. McFeely, L. Ley and D.A. Shirley, Chem. Phys. Lett. **29**, 491 (1974).

15. Y. Wang, M. Trenary, Chem. Mater. **5**, 199 (1993).

16. C.L. Perkins, M. Trenary, T. Tanaka, S. Otani, Surface Science **423**, L222 (1999).

17. B. D. Padalia, J. K. Gimzewski and S. Affrossman, W. C. Lang, L. M. Watson and D. J. Fabian, Surface Science **61**, 468 (1976).

18. B.A. Orlowski, B.J. Kowalski, Z. Golacki, T. Story, and R.L. Johnson, Acta Physica Polonica **A88(5)**, 857 (1995).

19. B.A. Orlowski, E. Guziewicz, E. Nossarzewska-Orlowska , A. Bukowski, and R.L. Johnson, Surf. Sci. **507**, 218 (2002).

20. A. J. Nelson, J.J. Adams, and K. I. Schaffers, J. Appl. Phys. **94(12)**, 7493 (2003).

Figure Captions

Figure 1.   Crystal structure of GdCOB

Figure 2.   XPS core-level spectra for GdCOB crystal and Gd-oxide model compound (a)

Gd $3d_{5/2,3/2}$ and (b) Gd $4d_{5/2,3/2}$.

Figure 3.   XPS core-level spectra for GdCOB crystal and oxide model compounds (a) B

1s and (b) O 1s.

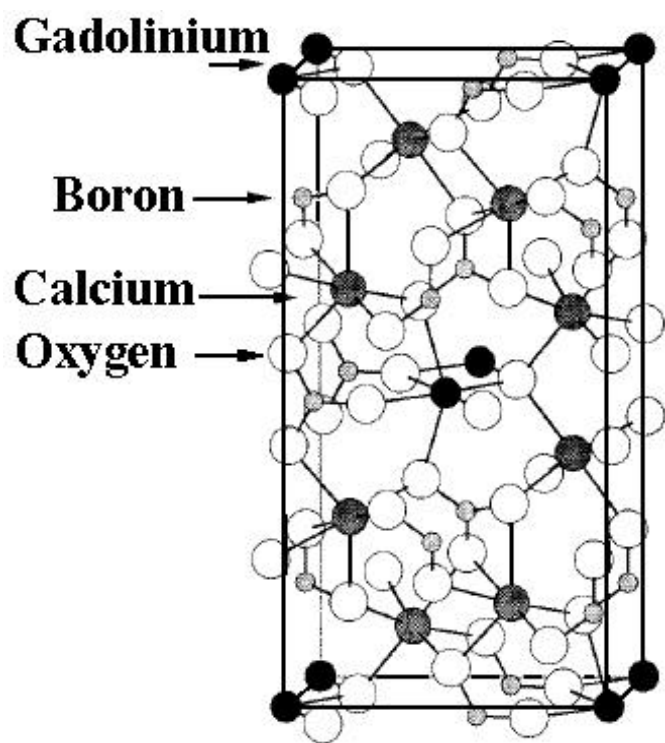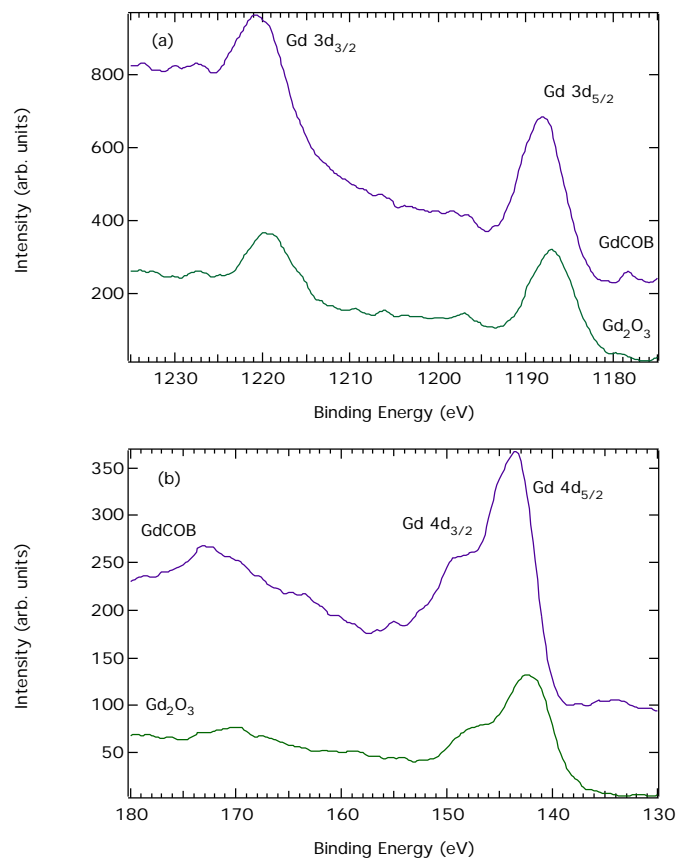Figure 4.   XPS valence band spectra for the GdCOB crystal and the oxide model
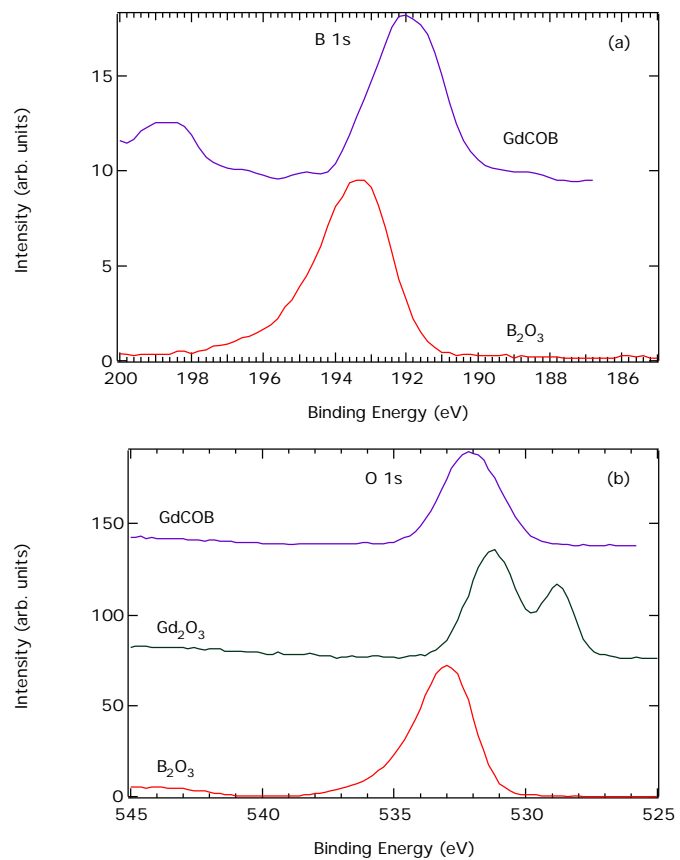
compounds.
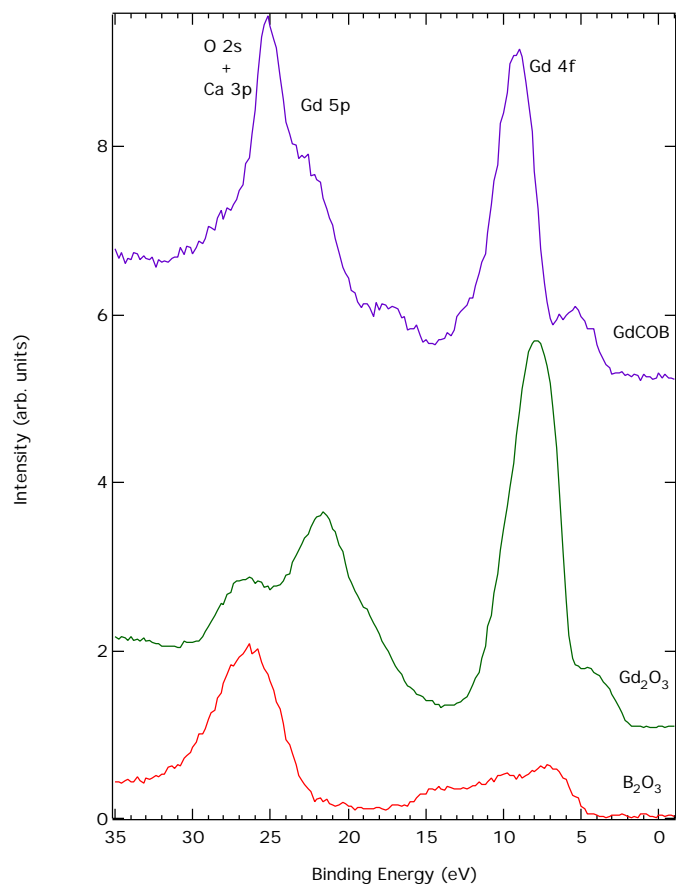
Figure 1.

Figure 2.

Figure 3.

Figure 4.